# Autosub Long Range: A Long Range Deep Diving AUV for Ocean Monitoring

Maaten E. Furlong, Dave Paxton, Peter Stevenson,
Miles Pebody, Stephen D. McPhail, and James Perrett
Marine Autonomous and Robotics Systems (MARS)
National Oceanography Centre
Southampton, UK

***Abstract*—This paper introduces the Autosub Long Range Autonomous Underwater Vehicle being developed at the National Oceanography Centre, Southampton. This propeller driven vehicle is designed to have a 6000m depth rating and a 6000km range. This is achieved by reducing the propulsion power by travelling slowly and hotel power by careful component selection and husbanding of resources. The challenges associated with net buoyancy compensation and low Reynolds number phenomena are outlined, and a passive compensation scheme is described. Early field trials are discussed, and the AUV's role in the upcoming FASTNEt science programme is outlined.**

## I. Introduction

The world oceans have always held a fascination for man, and while the earliest voyages of discovery charted and surveyed the oceans it wasn't until the Challenger Expedition of the 1870's that a more rigorous examination began. Studying the oceans in detail is an enormous challenge as they comprise 71% of the planet's surface and only the top layer is easily surveyed remotely. Examining the vast expanse of the remainder of the oceans can only be done using instruments collocated with the site of survey. This measurement requirement to '*be there*' has meant that we only have brief glimpses in space and time of this underwater world, and the bulk of the oceans remain to be explored. And yet, as we move more economic activity into the oceans, and concern grows about anthropogenic impact, these brief glimpses are not enough and a more thorough knowledge of the oceans is required.

This more detailed knowledge can for example inform: telecommunication companies about potential geohazards along their cable route; oil companies about the geological and bathymetric structure around their oil and gas fields; and oceanographic scientists about the changing state of ocean flows due to changes in climate. This need for a deeper understanding of the world's oceans is difficult to meet using existing approaches as the cost are prohibitively high. Thus, there is an urgent need for lower cost methods of delivering the data.

Slow speed long endurance Autonomous Underwater Vehicles (AUVs) can provide part of the solution. For example, underwater gliders are now routinely used for oceanographic surveys as they provide excellent data through the upper water column (typically 0-1000m). However, current gliders are slow, limited in depth rating, must follow a yo-yo profile through the water-column, and have limit space and power for additional sensor. Although these limitations are being worked on with propeller driven hybrid gliders [1], and deep gliders [2] being built, this class of vehicle is still only one piece of the data collection jigsaw. A second piece is to use a new class of slow speed propeller driven AUVs as these have similar long range but are not limited to yo-yoing and have a greater speed range. An examples of this class of vehicle is MBARI's Tethys [3]. This is a relatively small man portable AUV with a 300m depth rating, and although it extends what can be done just by the glider fleet it is still limited in depth and range. Thus, there is a need for a deeper diving, longer range AUVs which have larger sensor payloads.

Such a vehicle would of necessity be larger than Tethys, and would fill a complementary, but separate, niche in the data collection challenge. Example missions for this type of AUV are: full depth survey of choke points in the ocean e.g. Drakes passage and the extended Ellett Line[4]; acting as an untether, self deploying mooring which could transit from the beach to the worksite, hold station profiling to full ocean depth, and then return for collection; or performing bathymetric surveys in remote locations by travelling in low power mode to the worksite, and then activating high power instruments (e.g. a sidescan sonar) surveying the site, and then returning at low power for collection.

The benefits of such a deep diving long range AUV resulted in the Natural Environment Research Council funding the National Oceanography Centre (NOC) to develop a vehicle of this class. Thus, Autosub Long Range (AutosubLR) was born. This paper gives an overview of the AutosubLR AUV and describes the challenges in creating this vehicle. The paper then outlines the results of early trials, and concludes with a description of the forthcoming FASTNEt science campaign.

## II. AutosubLR Overview and Mechanical Design

AutosubLR, has been designed to meet the following science requirements:

- Maximum Depth rating : 6000 m
- Maximum range : 6000 km
- Endurance : 6 months
- Speed range : 0.35–1.0 m/s
- Max Payload : 30 litres
- Max payload weight : 10 kg

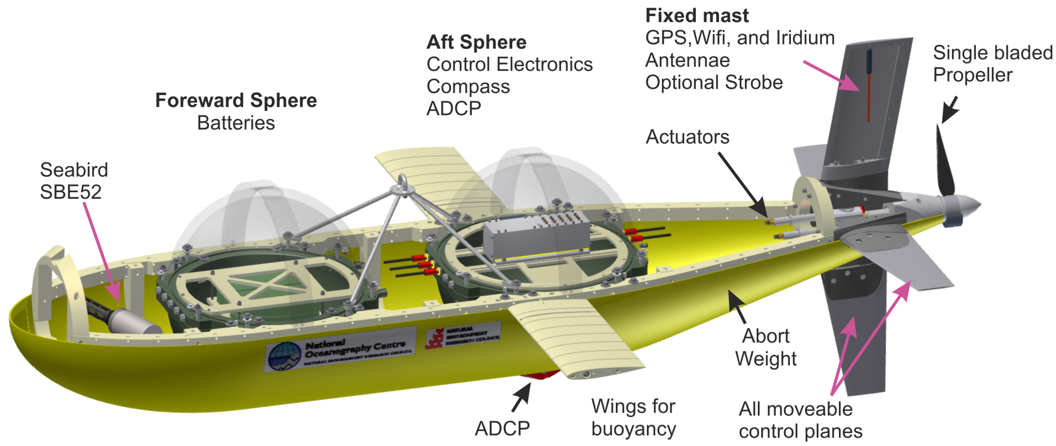


Fig. 1: An overview of AutosubLR based on a 3D CAD model of the vehicle

To achieve these goals we have developed an AUV (shown in Figure 1) which is 3.6m long, displaces 1.2 $m^3$ of water and has a dry weight of approximately 660 kg. A major factor in the size of the AUV is the 6000m depth rating and requirement for 6000km range. However, this size is not considered a significant issue as the vehicle is readily handled using a small ships crane.

The dry-space and buoyancy for AutosubLR is produced by two 6000m rated forged aluminium pressure spheres. The forward sphere contains the batteries for the vehicle, which are currently NiMH secondary cells to facilitate testing but will be upgraded to Lithium Primary cells for science missions. The rear sphere contains the control electronics, a PNI TCM XB compass/attitude module, and an RDI 300kHz ADCP. The ADCP is mounted through a hole in the bottom of the rear sphere to reduce the system weight by removing ADCP housing, and to remove the need wet for cabling, and hence removing a potential failure point. Forged pressure spheres were chosen for this design as: they are reliable (they do not have the pressure cycling issues associated with glass spheres); they provide considerable dry spaced for high energy density lithium primary cells; and suitable forgings were available at NOC. These NOC forgings have a large diameter, which has resulted in a relatively short fat vehicle.

The spheres are house in a plastic framework within the vehicle, and low density plastic materials are used throughout the AUV. This is both to save in-water weight, thereby increasing the battery payload, and to better match the compressibility of water. The plastic framework is strengthen by the fibreglass panels on the bottom and top of the AUV, and a single lifting point connected to the two spheres is used to lift the AUV from the water. An burn wire activated emergency drop weight system is also fitted in the tail of the AUV, which will drop its 7kg stainless steel weight if commanded or if the power fails.

Forward of the front sphere is a large internal space which contains a Seabird SBE-52 CTD sensors. This is a standard sensor for the AUV, and the depth sensor output is used as the depth input to the AUVs control system. There is also considerable room in the forwarwd space for mission depend payloads.

Propulsion power is provided by a custom designed propulsion unit which drives a single bladed propeller (both described in more detail later). The vehicle is manoeuvred using three all moveable conrol planes, while the top rudder is fixed and contains antennae for GPS, WiFi and Iridum as well as an optional strobe. The moveable control planes are controlled using custom acutators, similar in structure to the propulsion motor, that are installed along the fore-aft axis of the vehicle to simplify installation and removal. The output drive of the actuators goes through a worm and wheel gear to provide the 90° rotation required to drive the control planes. The control planes were sized so that the AUV would be stable in forward motion, and thus the control planes do not need to be continually adjusted to maintain heading.

The wings are designed to reduce the effect of the net buoyancy, and are made in sections so that they can be simply shortened or lengthened. They are also adjustable fore and aft and their angle of attack can also be modified. This allows the wings to be tuned for the desired mission characteristics.

The range for an AUV can be estimated using the following equation:

$$R = \frac{E}{P_P + P_H} \cdot V \quad (1)$$

Where, $E$ is the energy available in the system, $P_P$ is the propulsion power, $P_H$ is the total sensor and system power ('Hotel' power), and $V$ is the AUV forward speed. Although, the energy and hotel power can be readily calculated, determining propulsion power for a given forward speed is more challenging. For a neutrally buoyant craft travelling in a straight lined, the power can be determined by the vehicle drag multiplied by its forward velocity and divided by the efficiency of the propulsion system, or more specifically:

$$P_P = \frac{\left(\frac{1}{2}\rho V^2 \nabla^{\frac{2}{3}} C_{d_\nabla}\right) \cdot V}{\eta_{propulsion}} \tag{2}$$

Where, $\rho$ is the density of the water, $\nabla$ is the volume of the AUV, $C_{d_\nabla}$ is the volumetric drag coefficent for the vehicle and $\eta_{propulsion}$ is the total propulsion efficiency for the AUV. This, equation implicit assumes that $C_{d_\nabla}$ is independent of Reynolds number, and that the propulsion efficiency is constant. Unfortunately, neither is strictly true, but more critically the estimate of propulsion power ignores the effect of buoyancy. It has been previous shown how this buoyancy cannot be ignored for slow speed AUVs [5], and as the buoyancy has an impact on the range of the AUV, a method is needed to produce an estimate of its effect. Ideally one would have a detailed knowledge of how the energy per unit travelled at constant depth and buoyancy varied with speed. However, this is challenging to calculate, as it involves variation in: motor efficiencies at different power levels; propeller efficiencies at different Reynolds numbers and inflow angle; drag on the vehicle at different pitch angles; and the control plane angle (and hence drag) required to maintain level flight. As the data required for this calculation is not readily available an alternative *quick and dirty* method has been used.

First noting that the buoyancy force will require an equal and opposite lift from the AUV to maintain level flight, and then assuming that this lift is produced at a constant lift to drag ratio we can calculate the lift induced drag resulting from the net buoyancy. This, assumption gives a very crude model of the physics as the lift to drag ratio varies considerably with the angle of attack of the vehicle. However, it allows one to rapidly determine the scale of the effect of the buoyancy error on the range of the AUV. Revisiting equation 2 and in light of the above assumption the equation can be modify to take account of the buoyancy error ($\Delta B$), and thus becomes:

$$P_P = \frac{\left(\frac{1}{2}\rho V^2 \nabla^{\frac{2}{3}} C_{d_\nabla} + \Delta B \left(\frac{drag}{lift}\right)\right) \cdot V}{\eta_{propulsion}} \tag{3}$$

The range for various lift induced drags were calculated using equations 1 and 3 with the following estimated vehicle properties:

- Drag coefficient ($C_{d_\nabla}$) : 0.04
- Propulsion efficiency : 38%
- System power : 1 W
- On board energy : 20 KWHrs

The results presented in Figure 2 shows that even a small lift induced drag has a significant impact on the range of the AUV.

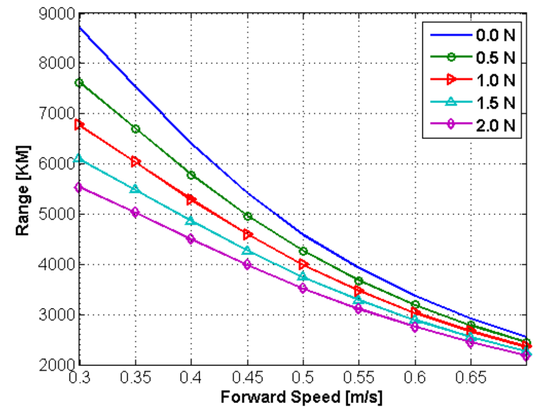


Fig. 2: AutosubLR range against speed for a series of lift induced drags

Thus, for AutosubLR to achieve its target range it must be very close to neutral buoyancy. This can be readily accomplished for local sea conditions, however, the density of seawater varies significantly on the scales that AutosubLR operates. This variation primarily results from the pressure increase as water depth increases, but it is also affected by the temperature variations in the water column, and very slightly by salinity variations. Unfortunately, AutosubLR's bulk modulus and temperature coefficient are different to that of sea water, so although the AUV can be trimmed correctly for a given pressure and temperature the net buoyancy will deviate considerably from this as the vehicle moves through the water column. To compound these problems the AUV also needs to have sufficient surface buoyancy to prevent wash-over of the antennae and associated communication problems. To alleviate these issues a buoyancy compensation system has been designed for the AUV.

### A. The Passive Buoyancy Compensation System

The buoyancy compensation system created for AutosubLR is passive in operation. It attempts to more accurately match the vehicle's bulk modulus to that of seawater, while still giving 20N of positive buoyancy at the sea surface. The target is to keep the net buoyancy between 0–20N for the bulk of the vehicle's operation. For safety reasons the AUV is currently designed not to go negatively buoyant. The buoyancy range target was chosen assuming a lift of drag ratio of 20, thus giving a maximum lift induced drag of 1N, and thereby allowing the AUV to achieve its 6000 km target range. This passive compensation system consists of three elements:

***Low Pressure Air Compensator***
This comprises three litres of air at five bar, and provides the high buoyancy needed at the surface, but quickly compresses under pressure.

***Oil Bladders***
This consist of 105 litre of silicon oil that compresses more quickly than sea water thereby compensates for the low compressibility of the vehicle. Unfortunately,

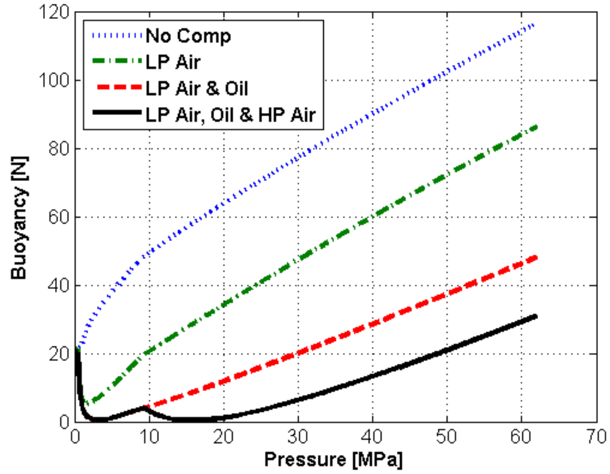


Fig. 3: Buoyancy vs pressure for AutosubLR with: no compensation; low pressure air compensation; low pressure air & oil compensation; low pressure air, oil & high pressure air compensation. All calculations assumed a mid latitude temperature profile.

the volume of oil required to optimally match the seawater cannot easily be contained in the vehicle.

***High Pressure Air Compensator*** This comprises two litres of air at 100 bar, and is used to compensate for buoyancy errors at deeper depths. Due to issues with high pressure gas storage this system would only be installed for specific deep missions.

The results of the buoyancy error vs. pressure are shown in Figure 3. Here the water density is calculated using EOS-80, and the temperature profile comes from page 23 Fig.2.6 of [6]. This varies the temperature from 19°C at the surface to 3°C at 62 MPa. The equation of state for the silicon oil has been determined experimentally by testing undertaken for the project, and the gas accumulators are modelled using the perfect gas law. Although this gas law over-predicts compression at high pressures this effect has been ignored in this analysis. The figure shows how the addition of the compensation elements to the AUV modifies its bulk modulus to more closely track the seawater.

The results show that the target net buoyancy is achieved using this setup for pressures to 49 MPa, which is acceptable for the majority of likely missions.

### B. Hydrodynamic Considerations

The shape of the vehicle is constrained by its two pressure spheres. These are faired to minimise drag and to provide space for the mission payload. Although the vehicle is short and fat with a length to diameter ratio of 4.5 this does not significantly affect the minimum volumetric drag ratio achievable [7].

Wings are also added to overcome the effects of the net positive buoyancy at slow speeds. Higher speed AUVs generate this lift by pitching down and using the hull as a large, but inefficient, lift surface. However, at slower speed this approach fails as it is not possible to generate sufficient lift and hence control authority is lost [5]. Also, before control authority is lost the lift induced drag becomes excessive due to the inefficiency of the lift generation. Thus, AutosubLR has been installed with large wings attached to the midsection of the vehicle.

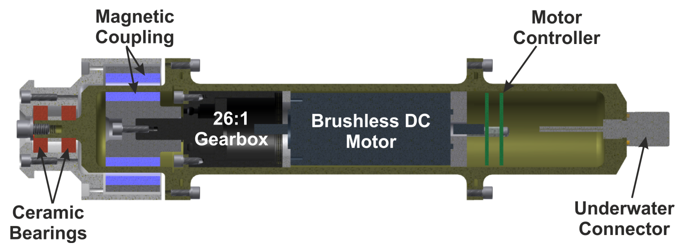


Fig. 4: Propulsion Motor Section View

These wings are based on a NACA0012 section, and have a chord of 300mm and a tip to root length of 640mm. To assess the performance at low speed it is important to consider the minimum Reynolds number at which they will be operating. At 0.4 m/s in 4°C sea water this is $\approx$ 75,000. This is low for a wing section and performance of the foil start to deteriorate below this speed due to the formation of a laminar separation bubble on the low pressure surface [8].

The control plane size is determined by the stability calculations for the AUV. These calculations were undertaken using a modified version of the component build up method outlined in [9]. As the minimum Reynolds number seen by the control planes was $\approx$ 37,500 midspan conventional aerofoil sections were inappropriate as the lift vs. angle of attack becomes highly non-linear due to the formation of laminar flow issues mentioned. Using the work of [8], we designed 'flat plate' control planes that consisted of a 5mm thick plate with a 5:1 elliptical leading edge and a trailing edge with a 3° taper. The control plane also tapers from 250mm at the root to 125mm at the tip. The wing root is clamped between two blocks which form a NACA0018 section at their root and then blend to the flat plate after 125mm. The two blocks sandwich the flat plate and clamp the control plane onto the actuator shaft.

### C. Propulsion System Design

An efficient propulsion system is essential for AutosubLR to achieve its desired long range. However, to achieve its maximum design speed of 1.0 m/s a motor capable of delivering over 60W is needed. As the efficiency of a motor tends to decrease with power output this high maximum power affects the low speed efficiency. The motor drive system, (Fig. 4), consists of a 6000m rated titanium pressure case containing the motor and drive electronics.

The main drive consists of a high efficiency brushless DC motor coupled to a 26:1 gearbox, which reduces the 24V no-load RPM from 3620 to 140 RPM. This reduced RPM is better suited for the propeller design, and the high torque and lower RPM also reduce the effect of coulomb friction and stirring losses in the power transmission. The output from the gearbox drives a magnetic coupling that transmits the motor torque to the propeller, which is mounted directly on the outer coupling. To minimise the frictional losses, the outer coupling is supported by two high quality ceramic bearings, which have very low rotational resistance and are impervious to corrosion.

A magnetic coupling was used to transmit the drive to the propeller for a number of reasons: firstly, there is no requirement to pressure balance the motor which would result in significant viscous losses; secondly, there is no need for dynamic seals which would increase the transmission losses and could fail; thirdly, housing the internals in a sealed dry space is inherently more reliable. The magnetic coupling design uses samarium cobalt magnets, for improved corrosion resistance, and has a 6 Nm breakout torque. The outer magnets coupling is also potted to prevent corrosion.

To minimise the wiring and connector size to the propulsion motor, a custom designed brushless dc motor controller was integrated into the housing. This high efficiency PIC18 based controller is designed to operate in conjunction with the main control computer thereby reducing the servicing of the motor controller, and in turn allowing the main processor to power down more regularly.

### D. Propeller Design

The final part of the propulsion system is the propeller. The primary challenge for this propeller design is the very low Reynolds number seen at the low cruising speeds. As noted previously, the performance of aerofoil sections degrades substantially at lower Reynolds numbers, and a similar trend is observed for propellers. In [10] 79 model aircraft propellers were tested at Reynolds number between 50,000–100,000, one of the thicker section propellers suffered a drop in efficiency from 42% at Re=100,000, to 28% at Re=50,000.

To alleviate this problem somewhat we took the unusual step of designing a propeller with a single blade. This doubles the propeller section Reynolds number compared to a twin blade propeller, while maintain the same blade area and similar thrust. Although the system is not dynamically balanced, the rotational speeds are low and hence the out of balance is not significant. The propeller is, however, hydrostatically balanced to produce a smooth torque load on the motor.

As noted above, the propeller section choice is crucial to achieving high propulsion efficiency at low Reynolds numbers. Classic propeller sections are not appropriate under these conditions, so an alternative approach was needed to find a suitable propeller section. Our method was to use Mark Drela's XFOIL program [11] to search through all available aerofoil sections listed in the UIUC Airfoil Database [12]. From this a suitable section was chosen for the propeller.

Having determined the propeller section, the inflow into the propeller disk was calculated by Dr Alex Phillips of the University of Southampton using commercial RANS software. This information was then combined with a propeller geometry file and inputted into the PALISUPAN panel code software [13] to estimate the thrust and torque coefficients of the propeller design. Once the final design was established, its geometry was imported into a commercial 3D CAD package for detailing, and was then sent out for manufacture. The propeller was initially manufactured in aluminium and anodised, but a recent prototype was created using the stereo lithography rapid prototyping process. This process was considerably quicker and cheaper than machining a custom propeller, and produced a lighter product that was easier to hydrostatically balance. However, the durability of the material when immersed in water for extended periods is unknown so further testing is required.

## III. Electronics and Software Architecture

The electronics and software system lie at the heart of the AUV. They must deliver the usual control requirements of a flight class vehicle (attitude control, navigation, power management, etc.) [14], and critically in this case they must do this at very low power levels with high reliability. High stability and reliability of the system is essential, and mean-time-between-failure of both the hardware and software components must reflect both the intended deployment time and the operational life of the AUV.

### A. Electronic Hardware

The control system hardware consists of a custom designed main board that hosts a TRITON270 miniature single board computer, which contains an Intel/Marvel PXA270 ARM based processor. Coupled to this main board are custom designed daughter boards which add serial interfaces, power management, RS485 outputs, GPS, and abort weight triggering. These subsystems, and the propulsion motor and actuators are built around PIC18 series microcontrollers and communicate with the TRITON270 via an RS485 serial bus.

Standard serial communications from the TRITON270 are used to interface the PNI TCM XB compass/attitude module, GPS receiver, SBE-52MP CTD sensor and the RDI 300kHz ADCP. External communications are via wireless 802.11 Ethernet and an Iridium satellite modem. Power switching and low power operation modes, including reduced PXA270 CPU clock frequency, for all these components are controlled by software on the TRITON270.

The Autosub Long-Range control system hardware presents a two layer architecture. Relatively simple low level processes are implemented on the PIC microcontrollers while the single TRITON270 centralised processor realises the higher level control and systems management functions.

### B. Software

The AutosubLR main control software runs within a Microsoft Windows CE 6.0 operating system, while the PIC18 based subsystems run native 'C' code. These subsystems run low level control and monitoring loops and are commanded using a mode and demand protocol similar to that implemented in previous Autosub AUVs [15].

The central control software consists of a primary process with execution threads that asynchronously manage mission command sequencing and actuator and sensor interaction. A central data structure implements a blackboard [16] architecture to allow data exchange between the various execution threads.

As AutosubLR moves relatively slowly and is directionally stable, the control loop does not have to be fast. Hence the main control process implements higher level functionality (i.e. navigation, depth control, position control, mission event processing, power management, system monitor and operator interaction) in a simple 1Hz 'sense-think-act' loop. It is also intended to slow this update rate during AUV cruise to allow the system to conserve power by switching to a low power state between processing cycles. The functional tasks executed by the main control process are:

1) Update sensor data
2) Read status data from the actuators
3) Process navigation
4) System status check
5) Process events
6) If triggered move to next action in the mission script sequence
7) Update actuation control functions, namely:
    a) Abort ballast control
    b) Propulsion control
    c) Sternplane control
    d) Rudder control
8) Log data
9) Status monitor update
10) Update the UI messaging
11) Power management (subsystem hibernation and sleep)

Communications between the AUV and operator are implemented using internet protocols such as TCP/IP, UDP/IP, and FTP. The main control process switches between an 802.11 wireless Ethernet connection for local communications and a point to point protocol (PPP) Iridium satellite link to a base-station computer.

The Autosub Long-Range AUV control system provides a basic functionality for a flight class AUV. Reliability and robustness are supported by the relatively simplistic control capability, and power consumption is reduced by the careful selection of components and the powering down and hibernation of systems between update cycles.

## IV. AutosubLR Field Trials and the FASTNEt Science Campaign

AutosubLR had its first field trials near the Canary Islands as part of the *RRS Discovery* D360 trials cruise held in January 2011. At this time the TRITON270 main control board communicated with the various subsystem using the $I^2C$ communication protocol. Unfortunately, there is a firmware issue with the $I^2C$ implementation in the TRITON270, and this coupled to noise on the communication lines resulted in the system periodically freezing up. Thus, only a limited range of the AUV's functionality was tested during this cruise.

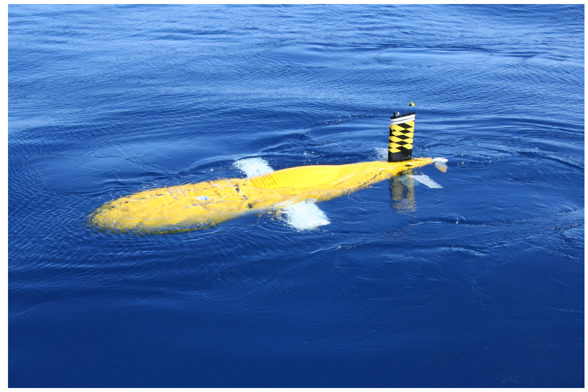

Fig. 5: AutosubLR waiting for recovery during its maiden sea-trials aboard *RRS Discovery* January 2011

The communication channel has since been revised to us RS485, and the AUV has subsequently been tested in Empress Dock which is located next to the oceanography centre. Although there is easy access to the dock, its limited size and depth coupled to the varying salinity levels due to its tidal nature has meant that only basic system checks on the new control system have been performed.

The testing has however, shown promise with the vehicle diving successfully, controlling to depth and heading, and showing stable flight. The maximum speed and the power usage at slower speeds have been worse than expected, but it is difficult to assess the size and cause of these issues due to the nature of the test site so further investigation is required.

The current focus for development is geared towards AutosubLR's role in the upcoming FASTNEt (**F**luxes **A**cross **S**loping **T**opography of the **N**orth **E**ast A**t**lantic). This NERC funded science programme will investigate interaction between the shelf seas and the deep ocean around the continental shelf of the UK. AutosubLR's role in this will involve five two month deployment of approximately 2,500 km in length and up to 1,500m in depth. The instrument payload for these missions are two RDI 600 kHz ADCPs (one upward the other downward facing), and a MicroRider-1000 turbulence profiler. The first science mission will occur in the summer of 2013, and preliminary trials of the system will be undertaken at Plataforma Oceanica de Canarias (PLOCAN) on Gran Canaria during January 2013.

## V. Conclusion

The paper has described the advantage of a new class of deep diving, long range AUV, and has introduced AutosubLR. This vehicle is designed to have a 6000m depth capability and a 6000km range. This is achieved by reducing the propulsion power of the AUV by travelling slowly, and reducing the hotel load by careful component selection and husbanding of resources. The challenges due to buoyancy variation and Reynolds number have also been highlighted and a passive buoyancy system to alleviate the problem has been described. A brief survey of the vehicle's initial trials has been given and the upcoming FASTNEt science missions have been described.

## ACKNOWLEDGMENT

The authors would like to thank the Natural Environment Research Council for their support in developing AutosubLR through the Oceans2025, National Capability and FASTNEt funding streams. We would also like to thank Leo Steenson, Alex Phillips for their assistance with the vehicle development.

## REFERENCES

[1] B. Claus, R. Bachmayer, and C. Williams, "Experimental flight stability tests for the horizontal flight mode of a hybrid glider," in *Autonomous Underwater Vehicles (AUV), 2010 IEEE/OES*, sept. 2010, pp. 1–6.

[2] T. Osse and C. Eriksen, "The deepglider: A full ocean depth glider for oceanographic research," in *OCEANS 2007*, 29 2007-oct. 4 2007, pp. 1 –12.

[3] Y. Zhang, M. Godin, J. Bellingham, and J. Ryan, "Using an autonomous underwater vehicle to track a coastal upwelling front," *Oceanic Engineering, IEEE Journal of*, vol. 37, no. 3, pp. 338 –347, july 2012.

[4] C. Holliday, "Extremes of Temperature and Salinity during the 1990's in the northern Rockall Trough: Results from the Ellett Line," in *ICES Symposium: Hydrobiological Variability in the ICES Area*, Edinburgh, Scotland, August 2001.

[5] M. E. Furlong, S. D. McPhail, and P. Stevenson, "A Concept Design for an Ultra-Long-Range Survey Class AUV," in *OCEANS 2007 - Europe*, June 2007, pp. 1–6.

[6] O. University, *Seawater: Its Composition, Properties and Behaviour*, ser. The Oceanography series. Elsevier Science, 1995.

[7] I. H. Abbott, "Airship model tests in the variable density wind tunnel," NACA, Tech. Rep. 394, 1932.

[8] E. V. Laitone, "Wind tunnel tests of wings at Reynolds numbers below 70 000," *Experiments in Fluids*, vol. 23, no. 5, pp. 405–409, 1997.

[9] E. V. Lewis, *Principles of naval architecture*, 2nd ed. Jersey City, N.J.: Society of Naval Architects and Marine Engineers, 1989, vol. III. Motion in Waves and Controllability.

[10] J. B. Brandt and M. S. Selig, "Propeller Performance Data at Low Reynolds Numbers," in *49th AIAA Aerospace Sciences Meeting*, AIAA Paper 2011-1255, Orlando, FL, January 2011, pp. 2011–1255.

[11] M. Drela, "XFOIL: An Analysis and Design System for Low Reynolds Number Airfoils," in *Conference on Low Reynolds Number Airfoil Aerodynamics*, University of Notre Dame, June 1989.

[12] UIUC Applied Aerodynamics Group (2010, Oct. $1^{st}$), *UIUC Airfoil Coordinates Database*. [Online]. Available: http://www.ae.illinois.edu/m-selig/ads/coord_database.html

[13] S. R. Turnock, "Technical manual and user guide for the surface panel code: PALISUPAN," University of Southampton, Southampton, UK, Tech. Rep. Ship Science Reports, 100, 1997.

[14] D. R. Blidberg, "The Development of Autonomous Underwater Vehicles (AUVs); A Brief Summary," in *ICRA*, Soeul, Korea, May 2001.

[15] S. D. McPhail and M. Pebody, "Navigation and control of an autonomous underwater vehicle using a distributed, networked, control architecture," *Journal of the Society of Underwater Technology*, vol. 23, pp. 19–30, 1998.

[16] S. A. Shafer, A. Stentz, and C. E. Thorpe, "An Architecture for Sensor Fusion in a Mobile Robot," in *IEEE International Conference on Robotics and Automation*, San Francisco, CA, April 1986.